Changes in bacterial community metabolism and composition during the degradation of dissolved organic matter from the jellyfish Aurelia aurita in a Mediterranean coastal lagoon

Marine Blanchet, Olivier Pringault, Marc Bouvy, Philippe Catala, Louise Oriol, Jocelyne Caparros, Eva Ortega-Retuerta, Laurent Intertaglia, Nyree West, Martin Agis, et al.

Changes in bacterial community metabolism and composition during the degradation of dissolved organic matter from the jellyfish *Aurelia aurita* in a Mediterranean coastal lagoon

Marine Blanchet [1,2], Olivier Pringault[3], Marc Bouvy[3], Philippe Catala[1,2], Louise Oriol[1,2], Jocelyne Caparros[1,2], Eva Ortega-Retuerta[1,2,4], Laurent Intertaglia[5,6], Nyree West [5,6], Martin Agis[3], Patrice Got[3], Fabien Joux[1,2*]

[1]Sorbonne Universités, UPMC Univ Paris 06, UMR 7621, Laboratoire d'Océanographie Microbienne, Observatoire Océanologique, F-66650 Banyuls/mer, France

[2] CNRS, UMR 7621, Laboratoire d'Océanographie Microbienne, Observatoire Océanologique, F-66650 Banyuls/mer, France

[3]UMR5119 Ecologie des systèmes marins côtiers (ECOSYM), CNRS, IRD, UM2, UM1; Université Montpellier 2. Case 093, F-34095 Montpellier Cedex 5, France

[4]Institut de Ciències del Mar, CSIC, Barcelona, Spain

[5]Sorbonne Universités UPMC Univ Paris 06, UMS 2348, Observatoire Océanologique, F-66650 Banyuls/Mer, France

[6]CNRS, UMS 2348, Observatoire Océanologique, F-66650 Banyuls/Mer, France

*corresponding author:

Email: joux@obs-banyuls.fr, Phone: 33(0)4 6888 7342, Fax: 33(0)4 6888 7395

Abstract

Spatial increases and temporal shifts in outbreaks of gelatinous plankton have been observed over the past several decades in many estuarine and coastal ecosystems. The effects of these blooms on marine ecosystem functioning, and particularly on the dynamics of the heterotrophic bacteria are still unclear. The response of the bacterial community from a Mediterranean coastal lagoon to the addition of dissolved organic matter (DOM) from the jellyfish *Aurelia aurita,* corresponding to an enrichment of dissolved organic carbon (DOC) by 1.4, was assessed during 22 days in microcosms (8 liters). The high bioavailability of this material led to (i) a rapid mineralization of the DOC and dissolved organic nitrogen from the jellyfish and (ii) the accumulation of high concentrations of ammonium and orthophosphate in the water column. DOM from jellyfish greatly stimulated heterotrophic prokaryotic production and respiration rates during the two first days, then these activities showed a continuous decay until reaching those measured in the control microcosms (lagoon water only) at the end of the experiment. Bacterial growth efficiency remained below 20%,

indicating that most of the DOM was respired and a minor part was channeled to biomass production. Changes in bacterial diversity were assessed by tag pyrosequencing of partial bacterial 16S rRNA genes, DNA fingerprints and a cultivation approach. While bacterial diversity in control microcosms showed little changes during the experiment, the addition of DOM from the jellyfish induced a rapid growth of *Pseudoalteromonas* and *Vibrio* species that were isolated. After 9 days the bacterial community was dominated by *Bacteroidetes*, which appeared more adapted to metabolize high-molecular-weight DOM. At the end of the experiment, the bacterial community shifted towards a higher proportion of *Alphaproteobacteria*. Resilience of the bacterial community after the addition of DOM from the jellyfish was higher for metabolic functions than diversity, suggesting that jellyfish blooms can induce durable changes in the bacterial community structure in coastal lagoons.

Keywords: *Aurelia aurita*, jellyfish, organic matter, heterotrophic bacteria, biodegradation, bacterial growth efficiency, bacterial diversity.

1. Introduction

Bacteria are key organisms in carbon cycling in aquatic ecosystems, acting as a sink (mineralization of dissolved organic carbon to CO_2) or as a link (production of biomass that can be transferred through the microbial food web) (Cotner and Biddanda 2002). The quality and the quantity of organic matter greatly influence bacterial metabolism and community structure (Azam and Malfatti 2007). The major autochthonous source of organic matter in the marine ecosystem comes from the phytoplankton, and a substantial part (10 to 50%) of primary production is channeled through bacteria (Cole et al. 1988). A number of field and experimental studies have indicated that DOM released during phytoplanktonic blooms was associated to important changes in the microbial community diversity and metabolic properties (e.g. McCarren 2010; Sarmento and Gasol 2012). Besides phytoplankton, DOM can be provided by jellyfish (used here to refer to medusa of the phylum Cnidarian and to members of the phylum Ctenophora) that can attain enormous biomasses in marine waters when the conditions are favorable (e.g. high nutrient concentrations) (Pitt et al. 2009, Purcell 2012).

The sudden appearance and disappearance of massive jellyfish blooms is one of the distinct features of this group (Condon et al. 2012). Top-down trophic control of jellyfish populations is low and jellyfish have been suggested as being a trophic “dead end” (Arai 2005).

Nonetheless, bacteria can recycle jellyfish biomass rapidly by different ways. Firstly, jellyfish release dissolved organic matter (DOM) by excretion and mucus production (Pitt et al. 2009). Secondly, during massive die-out events, jellyfish biomass sinks to the seafloor because dead animals have greater density than live animals (Yamamoto et al. 2008). The release rates of total organic carbon by dead jellyfish is significantly higher than that of living jellyfish (Pitt et al. 2009). Depending of the water depth, decomposition of dead jellyfish can occur in the water column or at the sediment surface. Rates of decomposition of both excretion and dead jellyfish biomass result in a large input of nutrients in the marine environment (Pitt et al. 2009; West et al. 2009; Tinta et al. 2010). Recent studies also reported a change in the bacterial structure in response to the use of organic matter from jellyfish for different coastal waters (Tinta et al. 2010; Condon et al. 2011; Tinta et al. 2012; Dinasquet et al. 2013).

Coastal lagoons are semi-enclosed systems occupying approximately 13% of the world's coastline with both marine and fluvial components (De Wit, 2011). The Mediterranean coast is bordered by a series of coastal lagoons with varying sizes, and some of them are associated with important economic activities (fisheries, aquaculture, tourism, recreation activities) (De Wit, 2011). Jellyfish blooms have been reported in these coastal lagoons and in particular were attributed to the scyphomedusa *Aurelia aurita* (Lo and Chen 2008; Lo et al. 2008; Bonnet et al. 2013). *A. aurita* is widespread in coastal and shelf sea environments around the world, predominantly inhabiting highly eutrophic waters where maximum abundance can reach 300 individuals.m^{-3} (Lo and Chen 2008). Due to the shallow depth of coastal lagoons, dead jellyfish can accumulate rapidly down to the sediment leading to hypoxic and anoxic conditions in these environments (West et al. 2009).

In the present study, we investigated the response of a Mediterranean coastal lagoon bacterial community to the addition of fresh jellyfish biomass (as DOM) of *A. aurita* using a microcosm approach. Our objective was to follow the changes in nutrients, bacterial activities and bacterial community structure during the total degradation of DOM from *A. aurita* in order to determine the resilience of the bacterial community exposed to the disturbance caused by a jellyfish bloom. For our purposes, we measured simultaneously bacterial production and respiration to determine the bacterial growth efficiency. We also combined the use of 454-tag pyrosequencing and DNA fingerprinting based on 16S rRNA genes and culture approach to characterize the bacterial diversity in response to the DOM addition from the jellyfish. To complete previous studies on this topic, we employed longer incubation period (22 days) with four sampling points allowing relevant analyses on the succession of taxa concurrent to the degradation of jellyfish DOM. Moreover, by using an incubation, long

enough to reach the complete mineralization of DOC from the jellyfish, it was possible to determine and then compare the resilience of bacterial functions and diversity after jellyfish DOM addition.

2. Material and methods

Preparation of dissolved organic matter from A. aurita

A. aurita jellyfish used in this study were produced in aquarium using *Artemia salina* nauplii as food (Lautan Production, Mèze, France). The jellyfish were less than 4 months old with a diameter around 8 cm. Twelve organisms were crushed with a blender. The homogenate was prefiltered onto 10-µm mesh (Nytex) and then filtered with a peristaltic pump onto 0.2-μm capsule filter (Polycap TC, Whatman) (previously rinsed with 10% HCl and washed thoroughly with Milli-Q water). The filtrate was recovered in a pre-combusted (450°C, 6 h) glassware bottle before being dispensed in the microcosms (see below).

Preparation of the microcosms and sampling

Water samples were collected in October 2010 from the shoreline of a Mediterranean coastal lagoon (Bages-Sigean, France, [42°36'21" N, 2°53'49" E]). The Bages-Sigean Lagoon covers 38 km^2 with a mean depth of 1.3 m and a maximal depth of 3 m. The catchment area covers greater than 456 km^2 and is drained by three rivers flowing into the lagoon. Water samples (salinity 33‰) were filtered sequentially by gravity onto 250, 100, 50 and 25 µm mesh (Nytex) and then onto 1-μm filter capsule (Polycap TC, Whatman) to remove fine particles. Six 10-L polycarbonate carboys (Nalgene) were filled with 8-L of the filtrated lagoon water. Three carboys received the DOM from *A. aurita* (300 ml) and the three other were used as controls. All the carboys were incubated in the dark at *in situ* temperature (18°C) under magnetic agitation. The caps of the carboys were maintained open to avoid any oxygen limitation. The microcosms were sampled 30 min after DOM addition (T0) and over 22 days (T22). At the last sampling, more than 60% of the initial volume was present in the microcosms.

Nutrients, dissolved organic carbon, nitrogen and phosphorus

Samples (60 ml) for nitrate (NO_3^-), nitrite (NO_2^-) and phosphate (PO_4^{3-}) were stored at -20°C and analyzed within 1 month of collection by colorimetry using a nutrient autoanalyzer (SEAL Analytical AA3HR) (Aminot and Kérouel 2007). Samples (100 ml in duplicate) for

ammonium (NH_4^+) were analyzed immediately according to Holmes (1999) with a fluorometer (Jasco). Samples (20 ml in duplicate) for dissolved organic carbon (DOC) were filtered through two pre-combusted (450°C, 6 h) 25-mm GF/F filters; the filtrate was transferred into precombusted glass tubes, poisoned with 85% H_3PO_4 (final pH=2), closed with Teflon lined screw caps and stored in the dark at room temperature until analysis. DOC was analyzed using the high temperature catalytic oxidation (HTCO) technique (Cauwet 1994) using a Shimadzu TOC-V analyzer. Prior to analyses and between each set of samples, an international certified reference sample for DOC concentration was analyzed to check the calibration of the analyzer and its stability over time.

Samples for dissolved organic nitrogen (DON) and phosphorus (DOP) were filtered through 2 pre-combusted (450°C, 6 h) 25-mm GF/F filters (Whatman). Samples were collected directly in Teflon bottles and immediately frozen (-20°C) until analysis. DON and DOP were simultaneously determined by the wet oxidation procedure (Pujo-Pay and Raimbault 1994). DON (±0.1 µM) and DOP (±0.02 µM) concentrations were determined by sample oxidation (30 min, 120°C) corrected for NH_4^+, NO_3^-+NO_2^- and PO_4^{3-} concentrations, respectively.

CDOM fluorescence

The fluorescence properties of colored dissolved organic matter (CDOM) were determined on samples filtered through 2 pre-combusted (450°C, 6 h) 25-mm GF/F filters (Whatman). Fluorescence was measured on a Perkin Elmer LS55 spectrofluorometer using a 1-cm quartz cuvette. Different excitation/emission couples were used to determine protein-like (275/340 nm) and humic-like (320/420 nm) compounds. Fluorescence intensity values were calibrated using the Raman scatter peak of Milli-Q water (Lawaetz and Stedmon 2009).

Virus count

Samples (2 ml) were fixed with 0.02 µm filtered formaldehyde (0.5% final concentration) and stored at -80°C after flash freezing in liquid nitrogen. Samples were filtered onto 0.02-µm filters (Anodisc, 25 mm diameter; Whatman) and virus-like particles (VLP) were stained on the filters using SYBR-Green I and enumerated under a Zeiss Axiophot microscope equipped for epifluorescence microscopy as previously described (Noble and Fuhrman 1998). At least 400 VLP were counted per filter in several randomly selected microscopic fields.

Heterotrophic prokaryotes abundance, production and respiration

Heterotrophic prokaryotic (including Bacteria and Archaea) abundance (HPA) was determined by flow cytometry. Duplicate 3 ml samples in cryovials were preserved with 0.2

µm filtered formalin (2% final concentration). The samples were gently mixed and left in the dark at room temperature for 10 min before quick-freezing in liquid nitrogen and storing at -80°C. The samples were later thawed at room temperature, stained with SYBR Green I (final concentration 0.025% (v/v) of the commercial solution; Molecular Probes Inc., OR) for at least 15 min at 20°C in the dark and analyzed on a flow cytometer (FACScan, Becton Dickinson, San Jose, CA) equipped with a 488 nm, 15 mW argon laser. HP cells were detected on a plot of green fluorescence (515-545 nm) *versus* right angle light scatter (SSC), using the green fluorescence as threshold parameter. Fluorescent beads (1.0 µm; Polysciences Inc., Warrington, PA) were added to each sample analyzed to normalize SSC and green fluorescence. HP growth rate (µ, d^{-1}) was calculated from the following equation $\mu = (\text{Ln } HPT_2 - \text{Ln } HPT_1) / (T_2-T_1)$. Generation time (g, h^{-1}) was determined as $g = (\text{Ln}(2) \times 24) / \mu$.

Heterotrophic prokaryotic production (HPP) was measured by ^{3}H-thymidine incorporation applying the centrifugation method (Smith and Azam 1992). Samples (1 ml in triplicate) were incubated in the dark at 18°C for 1 h with 20 nM [^{3}H]-thymidine (specific activity 83.2 Ci $mmole^{-1}$, Perkin Elmer) in 2 ml microtubes. Incorporations were terminated by the addition of trichloroacetic acid (TCA) to a final concentration of 5%. One killed control was prepared for each assay by the addition of TCA 15 min before the addition of ^{3}H-thymidine. Samples were stored for at least 1 h at 4°C and then centrifuged for 15 min at 12,000 g. The precipitate was rinsed twice with 5% TCA. The precipitates were resuspended in 1.0 ml of liquid scintillation cocktail (FilterCount, Perkin Elmer) and radioactivity determined by liquid scintillation counter (LS 5000CE Beckman). Thymidine incorporation rates were converted into carbon production using the conversion factors of 2.10^{18} cells produced by mole of thymidine incorporated and 20 fg C by cell (Ducklow and Carlson 1992).

Heterotrophic prokaryotic respiration (HPR) was measured at each time point using an oxygen microelectrode (Briand et al. 2004). The microprobes (Unisense, Denmark) are designed with an exterior guard cathode, which results in extremely low oxygen consumption by the electrodes ($4.7–47 \times 10^{-7}$ µmol O_2 h^{-1}). Probes have a response time shorter than 1 s and a precision of 0.05%. The HPR was measured over 4 h to 24 h in duplicate samples for each microcosm, placed in microchambers (2 ml) and immerged in a water bath with controlled temperature (18°C). A specific measurement of the dissolved O_2 concentration was carried out with a minimum of 4 times during incubation in microchambers. HPR was deduced from the linear regression established on these points of measurement. HPR were expressed in mgC m^{-3} d^{-1} using a respiratory quotient of 1 (del Giorgio and Cole 1998). We assume here that most of the respiration measured came from heterotrophic prokaryotes

because the water was filtered on 1-µm at the start of the experiment. However, we cannot exclude the growth of protozoa then after, leading to an overestimation of HPR. Bacterial growth efficiency (BGE, %) was calculated from the following equation BGE= HPP/(HPP+HPR).

Bacterial DNA extraction

Samples (500 ml) at T0, T2, T9 and T22 were filtered onto a 0.2 µm Sterivex filter (Durapore, Millipore) and stored at -80°C. For analysis, 840 ml of alkaline lysis buffer (50 mM Tris hydrochloride pH 8.3, 40 mM EDTA and 0.75 M sucrose) was added in the Sterivex. Cell lysis was accomplished by an initial incubation for 45 min at 37°C after adding 50 ml of freshly prepared lysozyme solution (20 mg ml^{-1}), and a second incubation at 55°C for 1 h after adding 100 ml of 10% sodium dodecyl sulfate and 10 ml of proteinase K (20 mg ml^{-1}). Six hundred ml of lysate was treated with 10 µl of a 100 mg ml^{-1} RNase A solution (Qiagen) before DNA extraction with the All Prep DNA/RNA mini (Qiagen) according to the manufacturer's instructions.

Analysis of bacterial community structure by capillary electrophoresis SSCP-based single strand conformational polymorphism (CE-SSCP) analysis

CE-SSCP fingerprinting was performed (i) to follow the changes in total bacterial community structure and (ii) to check the reproducibility between replicate microcosms. DNA was used as a template for PCR amplification of the variable V3 region of the 16S rDNA (*Escherichia coli* positions 329-533), as previously described (Ghiglione et al. 2005). CE-SSCP was performed using the ABI 310 Genetic Analyzer (Applied Biosystems), equipped with a capillary tube (47 cm × 50 mm) filled with a polymer mix composed of 5.6% GeneScan polymer (Applied Biosystems), 10% glycerol and 1× buffer with EDTA (Applied Biosystems). The similarity of the CE-SSCP profiles was assessed using the software SAFUM (Zemb et al. 2007), which normalized the total area of the profiles and mobilities between different runs using an internal standard. SAFUM renders a profile of fluorescence intensity as a function of retention time per sample, thus taking into account the presence and intensity of each individual signal. Ordination of Bray-Curtis similarities among normalized sample profiles was calculated using PRIMER 5 software (PRIMER-E, Ltd., UK).

Analysis of bacterial diversity and community structure by pyrosequencing

Bacterial tag-encoded FLX amplicon pyrosequencing (bTEFAP) was performed using the universal bacterial primers guidelines targeting the V1 to V3 hypervariable regions of the

bacterial 16S rRNA gene: 27Fmod (5′-AGRGTTTGATCMTGGCTCAG-3′) and 519r (5′-GWATTACCGCGGCKGCTG-3) as described previously (Dowd and al. 2008). Initial generation of the sequencing library was accomplished by a one-step PCR with a total of 30 cycles using the HotStarTaq Plus Master Mix Kit (Qiagen, Valencia, CA) and amplicons originating and extending from the 27Fmod primer. Tag-encoded FLX amplicon pyrosequencing analyses were completed using the Roche 454 FLX instrument with Titanium reagents, and procedures were performed at MR DNA (Shallowater, TX, USA) following manufacturer's guidelines.

Sequences were processed and analyzed using the Mothur software version 1.33 (Schloss et al. 2009) with default settings excluding sequences <200bp. Sequences were denoised using the Mothur implementation of PyroNoise and SeqNoise. Chimeras were removed using Chimera Slayer (Haas et al. 2011). The resulting clean sequences were clustered using operational taxonomic units (OTUs) at a 97% sequence identity level using the UCLUST algorithm (Edgar 2010) and a representative sequence from each OTU was classified using the Ribosomal Database Project (RDP) classifier (Wang et al. 2007) using the SILVA training set. Taxonomic identification of the sequence reads (tags) followed the approach by Sogin et al. (2006) and Huse et al. (2010). All samples were clustered into operational taxonomic unit (OTU) at a distance of 0.03 (Ghiglione and Murray 2012). All OTU and diversity analyses were performed on the randomly re-sampled datasets using Mothur.

Culturable bacterial counts, isolation and 16S rRNA gene sequencing

Culturable heterotrophic aerobic marine bacteria were enumerated during the experiment at T0, T2, T9 and T22 by plating 100 µl of diluted (in sterile seawater) or undiluted samples on marine agar 2216 (MA, Difco, Detroit, Mich.). Cycloheximide (100 mg/L) was added to the media to inhibit fungal growth. All culture were incubated at 25°C in the dark during two weeks before counting the colony forming units (CFU).

The identification of the most representative culturable strains was performed for one of the replicate for each condition after two days of incubation. The colonies were categorized using morphologic characteristics. All the different morphotypes (colony morphology) were picked for two successive sub-culturing steps on MA to ensure purification. One colony of each isolate was then grown in marine broth media (MB, Difco, Detroit, Mich.) during 48h at 25°C under agitation (100 rpm). Each culture was cryopreserved in 5% dimethylsulfoxide or 35% glycerol at -80°C. For genomic DNA extraction, 2 ml of each liquid culture were spun down (10,000 x g, 3 min). DNA extraction, PCR and sequencing were done as previously described

(Fagervold et al. 2013). Partial 16S rRNA gene sequences were trimmed manually, double checked and dereplicated using the package Staden-GAP4 (Staden et al. 2003). For bacterial strain identification, each FASTA file was uploaded in Ez Taxon-e (Kim et al. 2012) and compared with the cultured bacterial strain database using BLAST (Basic Local Alignment Search Tool). Sequences were deposited in Genbank (NCBI) under the following numbers: MOLA851-858 and MOLA865-880 from enriched microcosms and MOLA859-864 and MOLA881-887 from control microcosms.

Statistical analyses

Statistical analysis of the effects of treatment on chemical and biological parameters was performed using a one-way analysis of variance (ANOVA) and post-hoc Tukey tests with repeated measures (i.e. microcosms) and assuming homoscedasticity and normality of the data. Statistical significance was set at $p = 0.05$ and analysis was computed using XLSTAT 2014.2 software (Addinsoft).

Bacterial community structures, either as number and area of the peaks in the CE-SSCP profiles or presence and abundance of OTU in the pyrosequencing data, were compared using ordination of Bray–Curtis similarities and used to build dendrograms by the unweighted-pair group method with arithmetic averages (UPGMA). A similarity profile test (SIMPROF, PRIMER 6) was performed on a null hypothesis that a specific sub-cluster can be recreated by permuting the entry species and samples. The significant branch (SIMPROF, $p < 0.05$) was used as a prerequisite for defining bacterial clusters.

The extent of the correlation of bacterial diversity analyzed by pyrosequencing for both conditions with the chemical parameters and the viral abundance was assessed by canonical correspondence analysis (CCA). CCA was performed with MVSP v3.12d software (Kovach Computing Service, Anglesey Wales). Relative abundances of OTUs were transformed with arcsin ($\times^{0.5}$) to normalize the distribution of the data as suggested by Legendre and Legendre (1998).

3. Results

Degradation kinetics of jellyfish dissolved organic matter

The water in the control microcosms (i.e. lagoon water without any addition) was characterized by a high concentration of dissolved organic carbon (DOC, 573 μM), nitrogen (DON, 50 μM) and phosphorus (DOP, 0.7 μM), underlying the eutrophic status of this

ecosystem (Fig. 1a,b,c). Addition of dissolved organic matter (DOM) from *A. aurita* provided 252 µM DOC, 85 µM DON and 3 µM DOP, increasing significantly (ANOVA, $p<0.05$) their initial concentrations by 1.4, 2.5 and 5.8 times, respectively, compared to the control microcosms. The C:N ratio of the DOM was significantly (ANOVA, $p<0.05$) lower in the enriched microcosms (6:1) compared to the control microcosms (12:1) due to the high protein content of the jellyfish.

The DOC from the jellyfish was consumed at a high rate during the first four days of incubation (57 µM d^{-1}) and then at a lower rate (5.6 µM d^{-1}) (Fig. 1a). In contrast, the DOC in the control microcosms was consumed at a constant and low rate (4 µM d^{-1}) during the entire incubation. At the end of experiment, the same concentration of DOC (500 µM) was noted in the control and the enriched microcosms (ANOVA, $p>0.05$). The DON and the DOP concentrations were measured less frequently in the microcosms (Fig. 1b,c). The DON concentration decreased by 67 µM during the nine first days and then remained almost constant in the enriched microcosms. In contrast the DOP concentration increased during the first two days and then decreased during the rest of the incubation. For both DON and DOP, we did not observe significant changes in the control microcosms (ANOVA, $p>0.05$). At the end of the experiment, 86% of the jellyfish-derived DON and 57% of the jellyfish-derived DOP were degraded. The C:N ratio of the DOM in the control was close to the enriched microcosms by the end of the experiment (10:1 and 9:1, respectively).

The initial concentrations of NO_3+NO_2 (5.5 µM), NH_4 (6 µM) and PO_4 (0.5 µM) in the control microcosms were low and remained stable during the experiment time (Fig. 1d,e,f). The addition of jellyfish biomass led to an enrichment factor by 1.7, 1.0, and 11 for NO_3+NO_2, NH_4 and PO_4, respectively. NO_3+NO_2 concentrations remained stable in enriched microcosms, with the exception of an increase (+ 4 µM) at the end of the experiment (Fig. 1d). This increase was only due to changes in NO_2 concentration (data not shown). We observed a continuous increase of NH_4 up to 100 µM at T9, followed by a plateau (Fig. 1e). PO_4 concentrations (Fig. 1f) evolved in an opposite way to the DOP concentrations in the enriched microcosms: after a decrease during the first two days, the concentration increased during the rest of the incubation mainly between the days 2 and 9.

Protein-like and humic-like components of DOM were characterized by their fluorescence properties (Fig. 2). Protein-like components measured in the control microcosms remained constant during the experiment (Fig. 2a). In contrast, the protein-like components in the enriched microcosms showed a rapid decrease during the first nine days until reaching the value measured in the control microcosms at the end of the experiment. The concentration of

humic-like components (Fig. 2b) was identical in both conditions, remaining almost constant during the experiment. However, we noticed a slight but significantly (ANOVA, $p<0.05$) higher concentration of humic-like components in enriched conditions compared to the controls after 15 and 22 days.

Effect of jellyfish DOM addition on viral abundance, bacterial abundance and metabolism

Virus abundance remained almost constant during the entire period of the experiment in both controls and enriched microcosms (Fig. S1). A small but significant difference was observed between the two conditions at T2 and T4, with higher virus abundance in microcosms enriched with DOM from *A. aurita* (ANOVA, $p<0.05$).

During the three first days, we measured a rapid bacterial growth without lag time after the DOM addition from *A. aurita* (Fig. 3a). The bacterial growth rates calculated on the basis of bacterial abundance between T0 and T3 were 1.44 d^{-1} and 0.48 d^{-1} in the enriched and the control conditions, respectively. A sharp decrease in bacterial abundance occurred at T4 in the enriched microcosms, leading to a value identical to the control condition. Then, the bacterial abundance remained almost constant for the rest of the experiment.

A rapid increase in bacterial production (BP) and bacterial respiration (BR) was also observed in the enriched condition during the first days (Fig. 3b,c). After 3 days, both activities slowly decreased at a constant and similar rate during the rest of the experiment. After 22 days, the BP and BR were not significantly different between the control and the enriched microcosms (ANOVA, $p>0.05$).

Bacterial growth efficiency (BGE) calculated on the basis of bacterial production and respiration was quite low at the start of the experiment (<1%) (Fig. 3d). During the first 9 days, the BGE increased up to 17% in the microcosms enriched with DOM from *A. aurita*. The BGE measured in the control microcosms remained lower than the enriched microcosms until day 15, when both conditions presented the same mean value (13%).

Changes in culturable heterotrophic bacteria counts and diversity

At the start of the experiment, culturable bacteria represented only a small part of the total bacteria (0.25%) (Fig. 4). After two days of incubation, culturable bacteria accounted for 65% of total bacteria in enriched microcosms, compared to 3% in the control microcosms. The bacterial growth rate calculated on the basis of culturable bacteria counts during this period was 4.8 d^{-1} in the enriched condition compared to 1.92 d^{-1} in the controls. After 9 days, there was a significant difference in the culturable bacteria fraction between the two conditions (2%

and 12%, for control and enriched microcosms, respectively) (ANOVA, $p<0.05$). At the end of the experiment, the culturable bacteria fraction accounted for the same percentage (~10%) in both control and enriched microcosms.

Most of the culturable strains isolated after 2 days from an enriched microcosm, belonged to the *Pseudoalteromonas* and *Vibrio* genera (class of *Gammaproteobacteria*) (Table 1). After 22 days, a clear shift in culturable diversity was observed in this microcosm, with the dominance of *Flavobacteriaceae* (phylum of *Bacteroidetes*) and *Rhodobacteraceae* (class of *Alphaproteobacteria*). Even if the number of bacterial strains isolated from the control microcosm was less important than for enriched microcosm (6 versus 18), the diversity seemed to be more stable during the experiment with a majority of *Rhodobacteraceae*.

Changes in bacterial community structure induced by Aurelia-derived DOM

A similarity dendrogram based on CE-SSCP data showed a clear separation of the bacterial community diversity into four distinct clusters (Fig. 5a). With the exception of the microcosm C2 which presented outliers at T0 and T2, cluster I included the community profiles from control and enriched microcosms at T0, and cluster II grouped together the control microcosms at T2, T9 and T22. The later time points for the enriched microcosm clustered apart from the two clusters into two subclusters comprised of time point T2 (III) and T9, T22 respectively (IV). The bacterial community structure observed in the control microcosms remained closer to the initial bacterial structure than to the enriched microcosms. With the exception of microcosm C2, the replicate microcosms grouped together for a specific condition and time, indicating that the diversity changes observed between conditions or over the time are robust.

To analyze in more detail the composition of the bacterial community, pyrosequencing was performed on one replicate microcosm for each condition at different sampling times (Fig. 5a in bold). A total of 76,027 partial 16S rRNA gene sequences remained after quality controls, yielding on average 9,503 reads per sample (5,080 - 11,600). The number of sequences was normalized to 5,080 per sample (i.e., the lowest number of sequences obtained for a sample). The total of unique OTUs was 2,800 in the whole dataset (at 97% similarity). The rarefaction curves for all samples did not reach a plateau (Fig. S1). Hence, our sequencing effort did not cover completely the bacterial diversity. However, the shape of the rarefaction curves was similar for all samples allowing the comparison of these samples. The taxonomic richness based on the Chao1 index was slightly lower in the enriched microcosm at T0 and T2 compared to the control microcosm, and higher at T9 and T22 (Table 2). The diversity based

on the inverse Simpson index ($1/\lambda$) ranged from 3.6 to 35.2. The diversity was higher in the enriched condition at T0 compared to the control condition then lower at T2 and T9, and similar at T22. Both conditions showed a transient decrease in diversity at T9 (Table 2).

A dendrogram based on Bray-Curtis similarities using the total number of OTUs was similar to that observed with the DNA fingerprint approach (Fig. 5b). The samples at T0 (with or without the addition of DOM from *A. aurita*) grouped more closely with the samples from the control microcosms at T2, T9 and T22. No significant difference (SIMPROF test, $p > 0.05$) was observed between the samples in the control microcosms at T0 and T9. In contrast, a rapid shift in diversity was observed in the enriched microcosm at T2 (85% dissimilarity). After T9, the diversity tended to stabilize in this microcosm and no significant difference was observed in the bacterial structure at T22 (SIMPROF test, $p > 0.05$).

The community composition at the phylum level and proteobacterial subclasses varied between treatments and with time (Fig. 6). The changes in abundances described below refer to relative abundances of the sequences and do not refer to absolute abundances of the different bacterial groups. At T0, the enriched microcosm was characterized by a higher proportion of *Actinobacteria* (49% versus 19% in the control microcosm) and by a lower proportion of *Alphaproteobacteria* (16% versus 49% in the control microcosm). The control microcosm showed continuous changes over the experiment. At the end of the experiment, *Alphaproteobacteria* remained the most abundant taxon (67%), whereas the *Actinobacteria* and *Bacteroidetes* tended to decrease (1.4% and 12%, respectively). *Gammaproteobacteria* showed a transient increase at T9 (24%) to reach the initial percentage at the end of the experiment (8%). The bacterial community in the enriched microcosm was characterized by a high proportion of *Gammaproteobacteria* (65%) at T2, followed by a dominance of *Bacteroidetes* (77%) at T9. Finally, at T22, the *Bacteroidetes* decreased (46%) in favor of *Alphaproteobacteria* (36%) and *Plantomycetes* (5%).

Figure 7 shows the taxonomy information for the most abundant OTUs (i.e., present at a percentage higher than 1% in a specific sample). These 71 OTUs represented only 2.5% of the total number of OTUs, however their cumulative abundances represented between 52% and 88% of all the OTUs present in a specific sample. The majority of the *Alphaproteobacteria* sequences in the control microcosm were assigned to SAR11 throughout the experiment. *Actinobacteria* present in both the control and the enriched microcosms at T0 belonged to *Microbacteriaceae*. The bloom of *Gammaproteobacteria* at T2 was affiliated to *Pseudoalteromonas* and *Vibrio* species, and the *Bacteroidetes* at T9 were mainly composed of

Flavobacteriaceae. At the end of the experiment, the *Alphaproteobacteria* were dominated by *Roseobacter* clade bacteria (RCB) in the enriched microcosms.

In order to determine what factors were potentially controlling bacterial community composition, we applied a canonical correspondence analysis (CCA) to the data for both conditions (Fig. 8) using the distribution of the dominant OTUs (relative abundance >1%) determined by pyrosequencing. The variance explained by the two first axes represented almost 50 % (26.6% and 21.9% for axis 1 and 2, respectively). The first group comprising all the samples from the control condition and the sample at T0 from the enriched condition was related to none of chemical parameters or viral abundance. The sample at T2 from the enriched condition was isolated from the other clusters and dominated by the OTUs 0008 and 0014 (*Pseudoalteromonas*) and by the OTUs 0017 and 0027 (*Vibrio*). This group was positively structured by DOM and CDOM protein-like components. The third group including the samples at T9 and T22 from the enriched condition was dominated by the OTUs 0002, 0011 and 0021 belonging to the *Flavobacteriaceae* family and OTU0010 belonging to the *Roseobacter* genus. This cluster was positively related to inorganic nutrients, CDOM humic-like components and viral abundance.

4. Discussion

Processing of organic matter from the jellyfish and consequences for the system

If we estimate an average wet weight of 13 g per jellyfish (Lo and Chen, 2008) and apply the relationship between the wet weight and the organic carbon content determined by Schneider (1988) for *A. aurita*, the enrichment in DOM corresponded to the addition of the total biomass from one jellyfish in 11 L (i.e., 91 individuals m^{-3}). This value can be considered as high but not unrealistic (Lo and Chen 2008). After 22 days of incubation, the same DOC concentration was observed in the enriched and control microcosms suggesting that the bacterial community has degraded the entire DOC from *A. aurita*. This result highlights the high bioavailability of the DOM from *A. aurita* jellyfish as already reported by Tinta et al. (2012) and Purcell (2012). The excess of organic and inorganic nitrogen and phosphorus in the enriched microcosms at the end of the experiment suggests that the decrease of bacterial activities were mainly due to limitation by bioavailable carbon. In these conditions, the excess of DON and DOP after degradation of jellyfish DOM can persist in the system until a new pulse of labile organic carbon. The release of nutrients during the decomposition of organic matter from the

jellyfish observed in this study and others (e.g., West et al. 2009; Tinta et al. 2010; 2012) might stimulate primary production. However, high concentrations of ammonium, associated to unionized ammonia (NH_3), can be also inhibitory or toxic for some phytoplankton, amphipods, crustacean and fish species (Ferreti and Calesso 2011; Collos and Harrison 2012). The fact that only 14% DOC was degraded over 22 days in the control microcosm indicates that the bulk of DOC in coastal lagoons is refractory. The priming effect is a process well demonstrated in the case of soils that enhances the microbial decomposition of preexisting refractory organic matter upon addition of labile organic matter (Kuzyakov et al. 2000). During the decline of the bloom, jellyfish biomass can constitute a large reservoir of labile organic matter at the disposal of bacteria that can enhance the priming effect. Nevertheless, there was no evidence that DOM from the jellyfish helped for biodegradation of refractory DOM from the coastal lagoon (i.e., the final DOC and humic-like components concentrations in the enriched treatment were similar and higher, respectively, compared to the control treatment), suggesting that the priming effect did not occur under these experimental conditions. Recent studies on the priming effect in aquatic ecosystems gave contrasting results underlying the need for further studies on this process (Fonte et al. 2013; Bengtsson et al. 2014; Guenet et al. 2014).

In our study, DOM from *A. aurita* increased the BGE relative to the control condition after 4 days of incubation. In contrast, Condon et al. (2011) observed that the rapid increase of bacterial metabolism in response to the addition of DOM released by a jellyfish was accompanied by a significant decline of BGE by 10% to 15% compared to the control treatment. Dinasquet et al. (2013) observed a similar BGE (30-40%) for bacterial communities exposed or not to DOM from the ctenophore *Mnemiopsis leidyi*. These contrasting observations may result from differences in experimental setup and bacterial communities composition in these studies. Even if the BGE was stimulated with the presence of DOM from *Aurelia* in our study, its value remained relatively low (<20%) indicating that organic carbon was mainly shunted toward bacterial respiration rather than creation of new biomass. According to Condon et al. (2011), the low value of BGE induced by labile DOM from jellyfish could be explained by a inadequate organic C:N and C:P stoichiometry resulting in nongrowth energy dissipation (i.e., overflow metabolism). It must be underlined that for all these studies, the true value of the BGE remains questionable due to uncertainties in the different conversion factors used for its calculation, including the conversion factor for converting ^{3}H-thymidine uptake into bacterial carbon production (Kirschner et al. 2004) and the respiratory quotient that may change with substrate quality (Berggren et al. 2012).

Proteins which were identified as the major constituent of jellyfish are characterized by a RQ of 0.8. By lowering the value of RQ for jellyfish condition to 0.8, BGE was increased by 21% in average (range: 19.5%-24.4%). However, this modification did not change the general shape of the curve and the comparison with the control condition (data not shown). Moreover, the calculation of BGE is complicated because HPP and HPR were measured at different time scales: while the time of incubation of HPP was short (i.e., 1h), HPR required sometimes 24h of incubation. According to del Giorgio et al. (2011), this methodological aspect in activities measurements can introduce a bias for the BGE determination.

Dynamics of bacterial community structure during the degradation of DOM from A. aurita

Interpretation of diversity changes during incubation in microcosms is always questionable due to a potential bottle effect (Massana et al. 2001). The bottle effect may have occurred in our experiment, as observed by the changes in the culturable bacteria fraction in the control microcosms (0.2% at T0 and 10% at T22). However, diversity as measured by pyrosequencing and DNA fingerprinting indicated that the bacterial community structure in the control microcosms did not change as drastically as in the enriched microcosms. In addition, HPP and HPR did not show significant changes over time (ANOVA test, $p>0.05$) in the control incubation. Both observations suggest that even if bottle effect cannot be ruled out, consequences on diversity and functions were minor compared to the changes caused by the increase of DOM. The differences in the bacterial community structure at T0 revealed by pyrosequencing between the control and enriched microcosms may be explained by the introduction of bacteria in the microcosms with the DOM from *Aurelia*, even if the DOM was previously filtered on 0.2 µm. The high percentage of *Actinobacteria* found in these microcosms might be facilitated by the very small size of these bacteria allowing them to escape the filtration (Ghai et al., 2013).

The pyrosequencing and the DNA fingerprint data demonstrate the rapid and profound effect of DOM addition from *Aurelia* on the bacterial diversity changes that persisted until the end of the experiment. Our results confirm the major role played by *Gammaproteobacteria* during the first steps of DOM degradation from jellyfish as observed in other studies (Condon et al. 2011, Tinta et al. 2012, Dinasquet et al. 2013). Surprisingly, the *Pseudoalteromonas* and *Vibrio* species blooming in the enriched microcosms in the first days were not found in the ~5,000 sequences identified for each sample at the start of the experiment, suggesting that they belong to the rare biosphere (i.e., less than 0.1%) (Pedrós-Alió 2012). If we hypothesize that these species represent less than 0.02% (1 sequence on 5,000) of the 2.10^6 bacteria/ml

present at the start of the experiment, the theoretical bacterial growth rate for these bacteria during the three first days would be 4.32 d^{-1} (generation time = 3.8 h) to reach the concentration of 9.10^7 bacteria/ml measured in the enriched microcosms after 3 days. This bacterial growth rate is not unrealistic and is comparable to the value calculated on the basis of the culturable count. Tinta et al. (2012) also observed that culturable bacteria isolated during the degradation of organic matter coming from different jellyfish in Adriatic Sea belonged to *Gammaproteobacteria* with a dominance of strains affiliated to *Vibrionaceae* and *Pseudoalteromonadaceae*. *Vibrio* and *Pseudoalteromonas* species can rapidly outcompete other bacterial species in a context of high concentration of organic matter due to greater metabolic versatility and the presence of multiple copies of rRNA genes (Williams et al. 2011). Changes in bacterial composition may not result only from competition for organic matter, but also from sensitivity of bacterial species for antagonistic compounds. For instance, Titelman et al. (2006) reported that extracts from the scyphomedusa *Periphylla periphylla* can inhibit some bacterial species, including *Actinobacteria*. An antimicrobial peptide, aurelin, exhibiting activity against Gram-positive and Gram-negative bacteria has been also isolated from *A. aurita* (Ovchinnikova et al. 2006). Overall, the diversity index as revealed by pyrosequencing (Table 2) remained unchanged in enriched microcosms at T2. In contrast, Tinta et al. (2012) observed a reduction in the diversity of the bacterial community during the biodegradation of *A. aurita*. This difference could be explained by the lower number of 16S rRNA clone library sequences analysed in the study of Tinta el al. (2012).

Different reasons can be evoked to explain the sudden decrease in bacterial concentration in the enriched microcosms between T3 and T4 (94% less bacteria in one day). Viral infection can induce rapid changes in bacterial abundance in aquatic environments (Berdjeb et al. 2011). However, lytic infection is associated with the release of viruses in the environment. We did not observe significant changes in viral abundance during this period, suggesting that viruses were certainly not the main factor to explain the loss of bacteria observed. Protozoan grazing can be also a cause of bacterial abundance regulation. Most of the heterotrophic nanoflagellates (HNFs) were excluded at the start of the experiment by filtering the water on 1 µm but we cannot exclude the possibility that some smaller HNFs passed through the filter and then proliferated during the experiment. Unfortunately, we did not measure HNF abundance in our experiment to confirm this hypothesis. Even if the role of HNFs cannot be excluded, the bacterial loss rate measured during this period ($3.4\ 10^6$ bacteria/ml.h) seems particularly high (i.e., two orders of magnitude higher than grazing rates values reported in the sea [Jürgens and Massana 2008]); thus grazing by HNF was certainly not the only

explanation for the decreasing of bacterial cell numbers. An additional and not exclusive hypothesis, concerns the autolysis of bacteria after cessation of growth.

After the use of the most bioavailable DOM by *Gammaproteobacteria*, the bacterial community shifted towards a dominance of *Bacteroidetes* at T9. These bacteria are specialized in degrading polymeric organic matter compounds, including proteins (Fernández-Gómez et al. 2012). Interestingly, high proportion of *Bacteroidetes* have been reported in a Norwegian fjord where persistent high jellyfish biomass is observed (Riemann et al. 2006) and in association with the ctenophore *Mnemiopsis leidy* (water, tissue and gut) (Dinasquet et al. 2012). In our experiment, structural components of bacterial cells including membranes and peptidoglycan were certainly released in the microcosms during the bacterial decay of *Gammaproteobacteria* whatever the reason (protozoan grazing, viral infection or autolysis) (Nagata et al. 2003). *Bacteroidetes* have the capacities to recycle efficiently this material (Pinhassi et al. 1999; Cottrell and Kirchman 2000). Finally, we cannot exclude also the possibility that *Bacteroidetes* were favoured due to a negative selection by bacterivorous protists or viruses (Berdjeb et al. 2011). At the end of the experiment, there was an emergence of *Planctomycetes* (5% at T22). In aerobic environments, members of *Planctomycetes,* including the genera *Planctomyces* and *Rhodopirellula* identified in our study, have been reported to degrade complex organic matter into simpler compounds (Pizzetti et al. 2011).

Resilience of bacterial communities

Massive jellyfish blooms can be considered as a disturbance for the aquatic ecosystem. Stability is the general capacity of a community to return to equilibrium after perturbation, and includes components of resistance, recovery and resilience (Pimm 1984). Resistance is a community's ability to remain unchanged when challenged with disturbance. Recovery is a community's ability to return to its pre- disturbance composition or function, and resilience is the rate at which this return occurs (Shade et al. 2011). These different ecological concepts can be applied for a bacterial community exposed suddenly to the organic matter from jellyfish. Our results and others (Condon et al. 2011; Tinta et al. 2012; Dinasquet et al. 2013) showed that the resistance of bacteria is low, with rapid changes occurring in functions and structure when organic matter from a jellyfish is added (exudate or dead biomass). The determination of the recovery and the resilience needs experimental approaches sufficiently long to analyze these concepts. Most of the different studies previously performed on jellyfish biodegradation have used short-term incubations (<9 days) and ended before the complete degradation of organic carbon (dissolved or particulate) from the jellyfish (e.g., Condon et al.

2011; Tinta et al. 2012). In our study, it was possible to follow the complete degradation of DOC during the 22 days of incubation. Over this incubation we observed the recovery of the bacterial activities (production, respiration) but not for the bacterial structure (as measured by the Bray-Curtis distance), suggesting that resilience was higher for functions than for diversity. Consequently, jellyfish blooms can induce durable changes in chemistry (release of NH_4, DON and DOP) but also in the bacterial community structure of coastal lagoons. Future investigations on jellyfish blooms might be conducted in larger experimental systems (i.e., mesocosms) to measure at longer time scale these effects on different trophic levels by including both pelagic and benthic systems. This more realistic approach will also permit to explore the role of particle-attached bacteria in the jellyfish degradation, which was not considered in this study.

Acknowledgements

This study was supported by the CNRS-EC2CO program through the GELPROC project (2010-2012): "Interactions between gelatinous plankton and dynamics of prokaryotic communities". We wish to thank P. Roman for the jellyfish maintenance. We are grateful to the BIO2MAR platform (http://bio2mar.obs-banyuls.fr) for providing technical support and access to instrumentation. We thank the two anonymous reviewers for their comments that greatly improved the manuscript.

References

Arai MN (2005) Predation on pelagic coelenterates: a review. J Mar Biol Assoc UK 85:523–36.

Azam F, Malfatti F (2007) Microbial structuring of marine ecosystems. Nat Rev Microbiol 5:782-791.

Aminot A, Kérouel R (2007) Dosage automatique des nutriments dans les eaux marines. Méthodes en flux continu. Ifremer, MEDD, Quae (eds) (in French)

Bengtsson MM, Wagner K, Burns NR,. Herberg ER, Wanek W, Kaplan LA, Battin TJ (2014) No evidence of aquatic priming effects in hyporheic zone microcosms. Sci Rep 4:5187

Berdjeb L, Pollet T, Domaizon I, Jacquet S (2011) Effect of grazers and viruses on bacterial community structure and production in two contrasting trophic lakes. BMC Microbiol 11:88.

Berggren M, Lapierre J-F, P.A. del Giorgio (2012) Magnitude and regulation of bacterioplankton respiratory quotient across freshwater environmental gradients. ISME J 6:984–993.

Bonnet D, Molinero JC, Schohn T, Daly Yahia MN (2012) Seasonal changes in the population dynamics of *Aurelia aurita* in Thau lagoon. Cah Biol Mar 53:343–347.

Briand E, Pringault O, Jacquet S, Torréton J-P (2004) The use of oxygen microprobes to measure bacterial respiration for determining bacterioplankton growth efficiency. Limnol Oceanogr Methods 2:406–416.

Cauwet G (1994) HTCO method for dissolved organic carbon analysis in seawater: influence of catalyst on blank estimation. Mar Chem 47:55–64.

Cole JJ, Findlay S, Pace ML (1988) Bacterial production in fresh and saltwater ecosystems: a cross-system overview. Mar Ecol Prog Ser 43:1–10.

Collos Y, Harrison PJ (2012) Acclimation and toxicity of high ammonium concentrations to unicellular algae. Mar Poll Bull 80:8–23.

Condon RH, Steinberg DK, Del Giorgio PA, Bouvier TC, Bronk DA, Graham WM, Ducklow HW (2011) Jellyfish blooms result in a major microbial respiratory sink of carbon in marine systems. Proc Natl Acad Sci USA 108:10225–10230.

Condon RH et al. (2012) Questioning the rise of gelatinous. BioScience 62:160-169.

Cotner JB, Biddanda BA (2002) Small players, large role: microbial influence on biogeochemical processes in pelagic aquatic ecosystems. Ecosystems 5:105–121.

Cottrell MT, Kirchman DL (2000) Natural assemblages of marine proteobacteria and members of the Cytophaga–Flavobacter cluster consuming low- and high molecular-weight dissolved organic matter. Appl Environ Microbiol 66:1692–1697.

De Wit R (2011) Biodiversity of coastal lagoon ecosystems and their vulnerability to global change. In: Grillo O, Venore G (ed) Ecosystems Biodiversity. Tech Open Access Publisher pp 29–40

del Giorgio PA, Cole JJ (1998) Bacterial growth efficiency in natural aquatic systems. Ann Rev Ecol System 29:503–541.

del Giorgio PA, Condon R, Bouvier T, Longnecker K, Bouvier C, Sherr, E, Gasol JM (2011) Coherent patterns in bacterial growth, growth efficiency, and leucine metabolism along a northeastern Pacific inshore–offshore transect. Limnol Oceanogr 56:1–16.

Dinasquet J, Granhag L, Riemann L (2012) Stimulated bacterioplankton growth and selection for certain bacterial taxa in the vicinity of the ctenophore *Mnemiopsis leidyi*. Front Microbiol 3:302.

Dinasquet J, Kragh T, Schrøter M-L, Søndergard M, Riemann L (2013) Functional and compositional succession of bacterioplankton in response to a gradient in bioavailable dissolved organic carbon. Environ Microbiol 15:2616-2628.

Dowd SE, Callaway TR, Wolcott RD, Sun Y, McKeehan T, Hagevoort RG, Edrington TS (2008) Evaluation of the bacterial diversity in the feces of cattle using 16S rDNA bacterial tag-encoded FLX amplicon pyrosequencing (bTEFAP). BMC Microbiol 8:125.

Ducklow HW, Carlson CA (1992) Oceanic bacterial production. Adv Microb Ecol 12:113–181.

Edgar RC (2010) Search and clustering orders of magnitude faster than BLAST. Bioinformatics 26:2460–2461.

Fagervold SK, Urios L, Intertaglia L, Batailler N, Lebaron P, Suzuki MT (2013) *Pleionea mediterranea* gen. nov., sp. nov., a gammaproteobacterium isolated from coastal seawater Int J Syst Evol Microbiol 63:2700–2705.

Fernández-Gómez B, Richter M, Schüler M, Pinhassi J, Acinas SG, González JM, Pedrós-Alió C (2012) Ecology of marine Bacteroidetes: a comparative genomics approach. ISME J 7:1026–1037.

Ferretti JA, Calesso DF (2011) Toxicity of ammonia to surf clam (*Spisula solidissima*) larvae in saltwater. Mar Environ Res 71:189–194.

Fonte ES, Amado AM, Meirelles-Pereira F, Esteves FA, Rosado AS, Farjalla VF (2013) The combination of different carbon sources enhances bacterial growth efficiency in aquatic ecosystems. Microb Ecol 66:871–878.

Ghai R, Mizuno CM, Picazo A, Camacho A, Rodriguez-Valera F (2013) Metagenomics uncovers a new group of low GC and ultra-small marine Actinobacteria. Sci Rep. 3:2471.

Ghiglione JF, Larcher M, Lebaron P (2005) Spatial and temporal scales of variation in bacterioplankton community structure in the NW Mediterranean Sea. Aquat Microb Ecol 40:229–240.

Ghiglione JF, Murray AE (2012) Pronounced summer to winter differences and higher wintertime richness in coastal Antarctic marine bacterioplankton. Environ Microbiol 14:617–629.

Guenet B, Danger M, Harrault L, Allard B, Jauset-Alcala M, Bardoux G, Benest D, Abbadie L, Lacroix G (2014) Fast mineralization of land-born C in inland waters: first experimental evidences of aquatic priming effect. Hydrobiologia 721:35–44.

Haas BJ, Gevers D, Earl AM, Feldgarden M, Ward DV, Giannoukos G, Ciulla D, Tabbaa D, Highlander SK, Sodergren E, Methé B, DeSantis TZ, Petrosino JF, Knight R, Birren BW (2011) Chimeric 16S rRNA sequence formation and detection in Sanger and 454-pyrosequenced PCR amplicons. Genome Res 21:494–504.

Holmes RM, Aminot A, Kérouel R, Hooker BA, Petersen BJ (1999) A simple and precise method for measuring ammonium in marine and freshwater ecosystems. Can J Fish Aquat Sci 56:1801–1808.

Huse SM, Welch DM, Morrison HG, Sogin ML (2010) Ironing out the wrinkles in the rare biosphere through improved OTU clustering. Environ Microbiol 12:1889–1898.

Jürgens K, Massana R (2008) Protistan grazing on marine bacterioplankton. In: Kirchman DL (ed.) Microbial Ecology of the Oceans, 2nd edn. JohnWiley & Sons, Inc., Hoboken, New Jersey, pp 383-441

Kim OS, Cho YJ, Lee K, Yoon SH, Kim M, Na H, Park SC, Jeon YS, Lee JH, Yi H, Won S, Chun J (2012) Introducing EzTaxon: a prokaryotic 16S rRNA Gene sequence database with phylotypes that represent uncultured species. Int J Syst Evol Microbiol 62:716–721.

Kirschner AKT, Wihlidal P, Velimirov B (2004) Variability and predictability of the empirical conversion factor for converting ^{3}H-thymidine uptake into bacterial carbon production for a eutrophic lake. J Plank Res 26:1559–1566.

Kuzyakov Y, Friedel JK, Stahr K (2000) Review of mechanisms and quantification of priming effects. Soil Biol Biochem 32:1485–1498.

Lawaetz AJ, Stedmon CA (2009) Fluorescence intensity calibration using the Raman scatter peak of water. Appl Spectrosc 63:936–940.

Legendre P, Legendre L (1998) Numerical ecology, 2nd English edition. Elsevier Science BV, Amsterdam. Lo W-T, Chen IL (2008) Population succession and feeding of scyphomedusae, *Aurelia aurita*, in a eutrophic tropical lagoon in Taiwan. Estuar Coast Shelf Sci 76:227–238.

Lo W-T, Purcell JE, Hung J-J, Su H-M, Hsu P-K (2008) Enhancement of jellyfish (*Aurelia aurita*) populations by extensive aquaculture rafts in a coastal lagoon in Taiwan. ICES J Mar Sci 65:453–461.

Massana R, Pedrós-Alió C, Casamayor EO, Gasol JM (2001) Changes in marine bacterioplankton phylogenetic composition during incubations designed to measure biogeochemically significant parameters. Limnol Oceanogr 46: 1181–1188.

McCarren J, Becker JW, Repeta DJ, Shi Y, Young CR, Malmstrom RR, Chisholm SW, DeLong EF (2010) Microbial community transcriptomes reveal microbes and metabolic pathways associated with dissolved organic matter turnover in the sea. Proc Natl Acad Sci USA 107:16420–16427.

Nagata T, Meon B, Kirchman DL (2003) Microbial degradation of peptidoglycan in seawater. Limnol Oceanogr 48:745–754.

Noble RT, Fuhrman JA (1998) Use of SYBR Green I for rapid epifluorescence counts of marine viruses and bacteria. Aquat Microb Ecol 14:113–118.

Ovchinnikova TV, Balandin SV, Aleshina GM, Tagaev AA, Leonova YF, Krasnodembsky ED, Men'shenin AV, Kokryakov VN (2006) Aurelin, a novel antimicrobial peptide from jellyfish *Aurelia aurita* with structural features of defensins and channel-blocking toxins. Biochem Biophys Res Comm 348:514–523

Pedrós-Alió C (2012) The rare bacterial biosphere. Annu Rev Mar Sci 4:449–466.

Pimm SL (1984) The complexity and stability of ecosystems. Nature 307:321–326.

Pinhassi J, Azam F, Hemphala J, Long RA, Martinez J, Zweifel UL, Hagström A (1999) Coupling between bacterioplankton species composition, population dynamics, and organic matter degradation. Aquat Microb Ecol 17:13–26.

Pitt KA, Welsh DT, Condon RH (2009) Influence of jellyfish blooms on carbon, nitrogen and phosphorus cycling and plankton production. Hydrobiologia 616:133–149.

Pizzetti I, Fuchs BM, Gerdts G, Wichels A, Wiltshire KH, Amann R (2011) Temporal variability of coastal *Planctomycetes* clades at Kabeltonne Station, North Sea. Appl Environ Microbiol 77:5009–5017.

Pujo-Pay M, Raimbault P (1994) Improvement of the wet oxidation procedure for simultaneous determination of particulate organic nitrogen and phosphorus collected on filters. Mar Ecol Prog Ser 105:203–207.

Purcell JE (2012) Jellyfish and Ctenophore blooms coincide with human proliferations and environmental perturbations Annu Rev Mar Sci 4:1.1–1.27

Riemann L, Titelman J, Båmstedt U (2006) Links between jellyfish and microbes in a jellyfish dominated fjord. Mar Ecol Prog Ser 325:29–42.

Sarmento H, Gasol JM (2012) Use of phytoplankton derived dissolved organic carbon by bacterioplankton large phylogenetic groups. Environ Microbiol 14:2348–2360.

Schneider G (1988) Chemische zusammensetzung und biomasseparameter der ohrenqualle *Aurelia aurita*. Helgoländer Meeresunters 42:319-327.

Schloss PD, Westcott SL, Ryabin T, Hall JR, Hartmann M, Hollister EB, Lesniewski RA, Oakley BB, Parks DH, Robinson CJ, Sahl JW, Stres B, Thallinger GG, Van Horn DJ, Weber CF (2009) Introducing mothur: open-source, platform-independent, community-supported software for describing and comparing microbial communities. Appl Environ Microbiol 75:7537–7541.

Shade A, Read JS, Welkie DG, Kratz TK, Wu CH, McMahon KD (2011) Resistance, resilience and recovery: aquatic bacterial dynamics after water column disturbance. Environ Microbiol 13:2752–2767.

Smith DC, Azam F (1992) A simple, economical method for measuring bacterial protein synthesis rates in seawater using ^{3}H-leucine. Mar Microb Food Webs 6:107–114.

Sogin ML, Morrison HG, Huber JA, Welch DM, Huse SM, Neal PR, Arrieta JM, Herndl GJ (2006) Microbial diversity in the deep sea and the underexplored "rare biosphere". Proc Natl Acad Sci USA 103:12115–12120.

Staden R, Judge DP, Bonfield JK (2003). Managing sequencing projects in the GAP4 environment. Introduction to bioinformatics. A theoretical and practical approach. Krawetz SA, Womble DD (eds). Human Press Inc., Totawa, NJ 07512

Tinta T, Kogovsek T, Malej A, Turk V (2012) Jellyfish modulate bacterial dynamic and community structure. PlosOne 7:e39274.

Tinta T, Malej A, Kos M, Turk V (2010) Degradation of the Adriatic medusa *Aurelia* sp. by ambient bacteria. Hydrobiologia 645:179–191.

Titelman J, Riemann L, Sørnes TA, Nilsen T, Griekspoor P, Båmstedt U (2006) Turnover of dead jellyfish: stimulation and retardation of microbial activity. Mar Ecol Prog Ser 325:43–58.

Wang Q, Garrity GM, Tiedje JM, Cole JR (2007) Naive bayesian classifier for rapid assignment of rRNA sequences into the new bacterial taxonomy. Appl Environ Microbiol 73:5261–5267.

West EJ, Welsh DT, Pitt KA (2009) Influence of decomposing jellyfish on the sediment oxygen demand and nutrient dynamics. Hydrobiologia 616:151–160.

Williams T, Joux F, Lauro FM, Matallana-Surget S, Cavicchioli R (2011) Physiology of marine oligotrophic ultramicrobacteria. In: Horikoshi K, Antranikian G, Robb F, Stetter K, Bull AT (eds), Extremophiles handbook. Springer Verlag GmbH, Heidelberg, Germany, pp. 1179–1199

Yamamoto J, Hirose M, Ohtani T, Sugimoto K, Hirase K, Shimamoto N, Shimura T, Honda N, Fujimori Y, Mukai T (2008) Transportation of organic matter to the sea floor by carrion falls of the giant jellyfish Nemopilema nomurai in the Sea of Japan. Mar Biol 153:311–317.

Zemb O, Haegeman B, Delgenes JP, Lebaron P, Godon JJ (2007) SAFUM: statistical analysis of SSCP fingerprints using PCA projections, dendrograms and diversity estimators. Mol Ecol Notes 7:767–770.

Table 1. List of 16S rRNA sequences of bacterial colonies isolated in the control and enriched microcosms after 2 and 22 days of incubation with high similarity (>97%) to sequences previously reported.

Treatment, time incubation	Isolate	Closest relative strain in EZ biocloud	%similarity	Family	Isolation source
Control, 2 days	MOLA864	*Muricauda lutimaris*	100.00	*Flavobacteriaceae*	Tidal flat of the Yellow Sea
	MOLA860 (3 isolates)	*Lentibacter algarum*	100.00	*Rhodobacteraceae*	Coastal water during a massive green algae bloom
Control, 22 days	MOLA922	*Celeribacter neptunius*	99.75	*Rhodobacteraceae*	Tidal flat sediment
	MOLA888	*Phaeobacter arcticus*	98.31	*Rhodobacteraceae*	Arctic Ocean
	MOLA890	*Alteromonas tagae*	97.78	*Alteromonadaceae*	Estuary
	MOLA881	*Lentibacter algarum*	97.40	*Rhodobacteraceae*	Coastal water during a massive green algae bloom
DOM Aurelia, 2 days	MOLA855 (5 isolates)	*Pseudoalteromonas undina*	100.00	*Pseudoalteromonadaceae*	Seawater
	MOLA917	*Pseudoalteromonas issachenkonii*	100.00	*Pseudoalteromonadaceae*	Thallus of the brown alga *Fucus evanescens*
	MOLA857 (2 isolates)	*Pseudoalteromonas tetraodonis*	99.53	*Pseudoalteromonadaceae*	Pufferfish
	MOLA853	*Vibrio gigantis*	99.77	*Vibrionaceae*	Cultured oysters
	MOLA852	*Vibrio hemicentroti*	99.76	*Vibrionaceae*	Gut microflora of sea urchin
	MOLA850 (2 isolates)	*Vibrio lentus*	99.75	*Vibrionaceae*	Mediterranean oysters
	MOLA858	*Olleya marilimosa*	99.28	*Flavobacteriaceae*	Southern Ocean
DOM Aurelia, 22 days	MOLA874 (3 isolates)	*Pseudoalteromonas undina*	100.00	*Pseudoalteromonadaceae*	Seawater
	MOLA892	*Alteromonas tagae*	98.35	*Alteromonadaceae*	Estuary
	MOLA869 (4 isolates)	*Arenibacter palladensis*	99.53	*Flavobacteriaceae*	Green macroalga
	MOLA870	*Arenibacter echinorum*	98.48	*Flavobacteriaceae*	Sea urchin
	MOLA880	*Celeribacter baekdonensis*	99.75	*Rhodobacteraceae*	Tidal flat sediment
	MOLA889	*Phaeobacter gallaeciensis*	99.27	*Rhodobacteraceae*	Larval cultures of scallop
	MOLA879	*Sulfitobacter dubius*	98.50	*Rhodobacteraceae*	Star fish
	MOLA877	*Ruegeria scottomollicae*	97.88	*Rhodobacteraceae*	Marine electroactive biofilm
	MOLA878	*Phaeobacter caeruleus*	97.57	*Rhodobacteraceae*	Marine electroactive biofilm
	MOLA871 (2 isolates)	*Shimia biformata*	97.12	*Rhodobacteraceae*	Sea water
	MOLA867	*Novosphingobium pentaromativorans*	97.38	*Sphingomonadaceae*	Estuarine sediment

Table 2. Number of OTUs, microbial richness and diversity estimates based on randomly picked OTUs normalized to 5080 sequences per sample to accommodate for the sample with the lowest number of sequences.

	Control				+ DOM Aurelia			
	0	2	9	22	0	2	9	22
OTU number	557	960	343	774	484	569	579	878
Richness (Chao1)	1034	1164	782	1309	991	986	1219	1426
Diversity (Inverse Simpson)	8.2	35.2	8.7	22.6	14.8	13.9	3.6	21.1

Figure legends

Fig. 1. Dissolved organic carbon (DOC, a), dissolved organic nitrogen (DON, b), dissolved organic phosphorus (DOP, c), nitrates plus nitrites (NO_3+NO_2, d), ammonium (NH_4, e) and phosphate (PO_4, f) concentrations during the incubations. Each point represents three replicates (mean ± standard deviation). The initial enrichment factor (EF) between enriched and control microcosms is indicated for each parameter.

Fig. 2. CDOM fluorescence of protein-like (a) and humic-like substances (b) concentrations during the incubations (ru= Raman Units). Each point represents three replicates (mean ± standard deviation).

Fig. 3. Bacterial abundance (a), production (b), respiration (c) and growth efficiency (d) during the incubations. Each point represents three replicates (mean ± standard deviation).

Fig. 4. Percentages of Colony Forming Units (CFU) to total direct counts (flow cytometry) during the incubations. Each point represents three replicates (mean ± standard deviation).

Fig. 5. Dendrograms of similarity based on (a) DNA CE-SSCP fingerprints and (b) OTUs table from the 16S rDNA 454-tag sequences for control microcosms (C1, C2, C3) and enriched microcosms with DOM from *A. aurita* (A1, A2, A3) after 0, 2, 9 and 22 days of incubation (T0, T2, T9, T22). Clustering is on the basis of a distance matrix computed using the Bray–Curtis index of similarity. The dendrogram was inferred with the unweighted pair-group average algorithm (UPGMA). a: The clusters were numbered from I to IV. Samples selected for 454 pyrosequencing are indicated in bold. b: Red branches do not differ significantly (SIMPROF test, $p > 0.05$).

Fig. 6. Cumulative bar charts comparing the main relative phyla and Proteobacteria class abundances for control microcosms (A) and microcosms with DOM from *A. aurita* (B).

Fig. 7. Heatmap displaying the relative abundances of specific OTUs across the samples. Only OTUs with a contribution higher than 1% in the sample were used. Multiple OTUs with the same taxonomic assignment were numbered sequentially. The contribution of these OTUs to the total OTUs present in each sample is indicated at the bottom.

Fig. 8. Canonical correspondence analysis (CCA) of bacterial community structure (OTUs presented on Fig. 7) and chemical factors and viral abundance. The percent of explained variation is shown in brackets. The inflation factors for the analysis are given in Table S1.

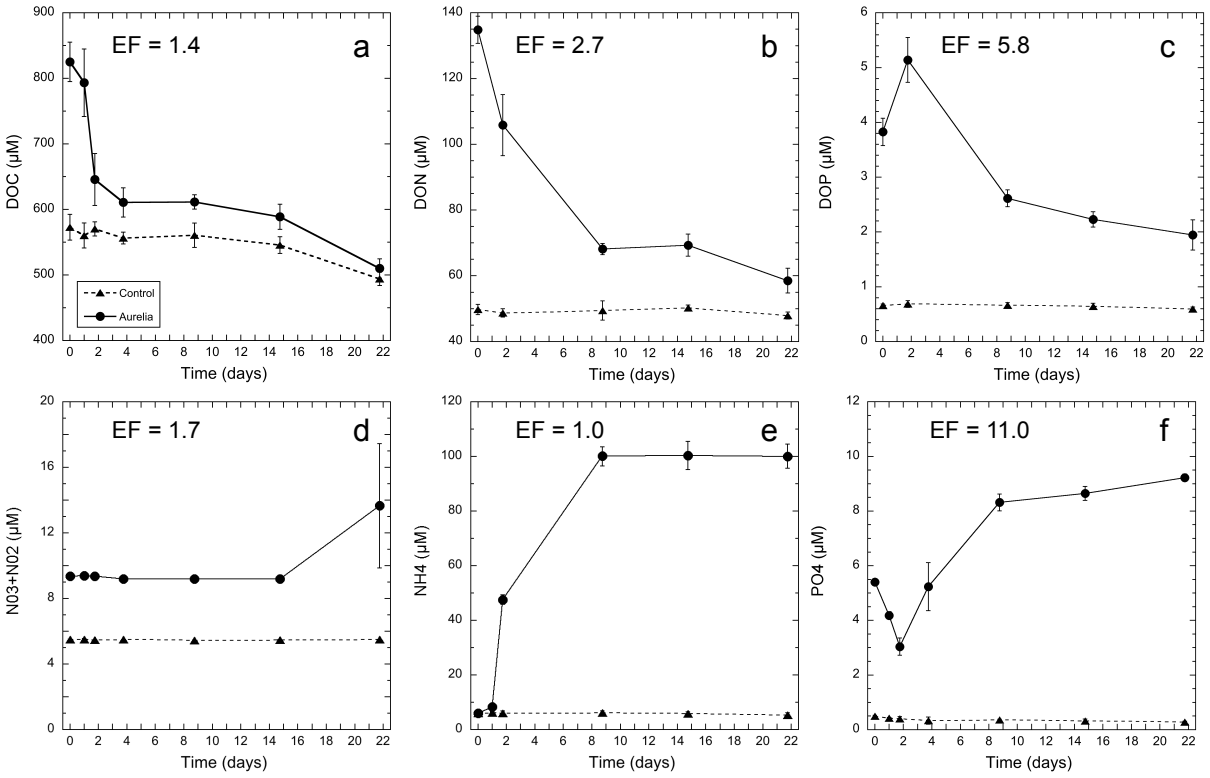
EF = 1.4
a
DOC (µM)
Control
Aurelia
Time (days)
EF = 2.7
b
DON (µM)
Time (days)
EF = 5.8
c
DOP (µM)
Time (days)
EF = 1.7
d
N03+N02 (µM)
Time (days)
EF = 1.0
e
NH4 (µM)
Time (days)
EF = 11.0
f
PO4 (µM)
Time (days)

Figure 1

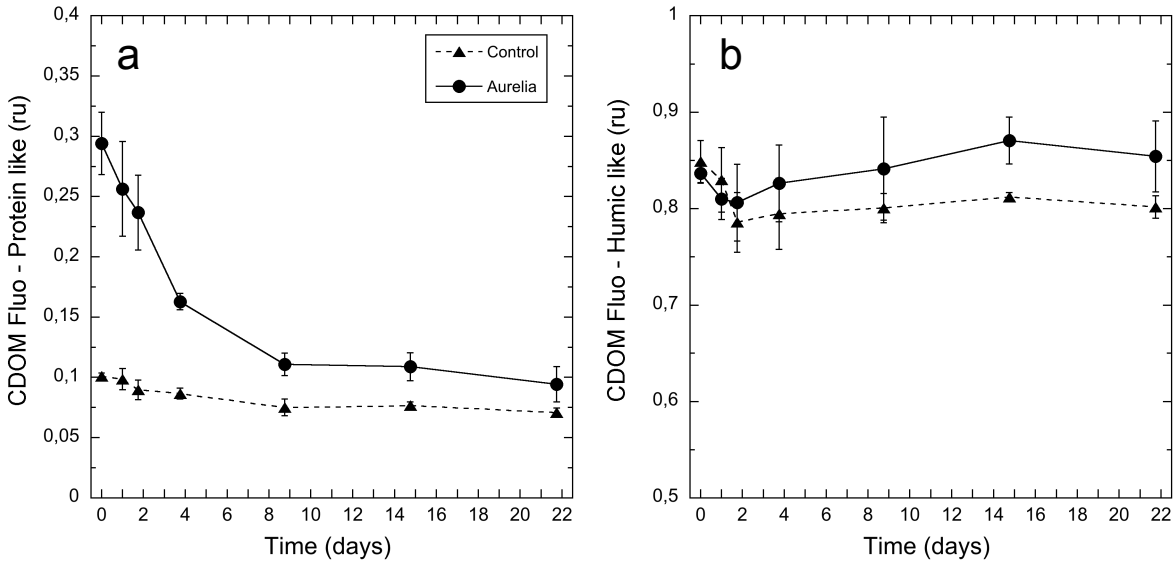
a
Control
Aurelia
CDOM Fluo - Protein like (ru)
Time (days)
b
CDOM Fluo - Humic like (ru)
Time (days)

Figure 2

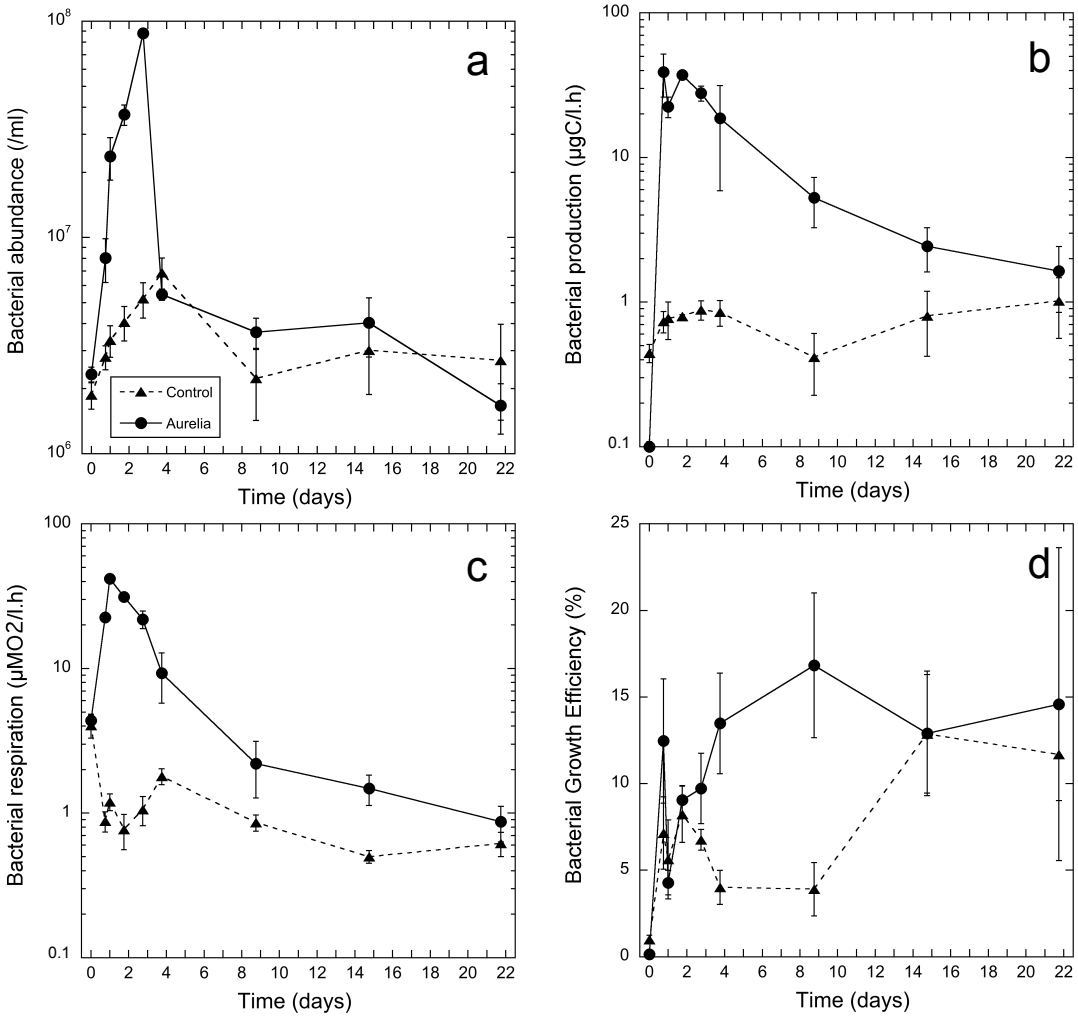
a
Bacterial abundance (/ml)
Control
Aurelia
Time (days)
b
Bacterial production (µgC/l.h)
Time (days)
c
Bacterial respiration (µMO2/l.h)
Time (days)
d
Bacterial Growth Efficiency (%)
Time (days)

Figure 3

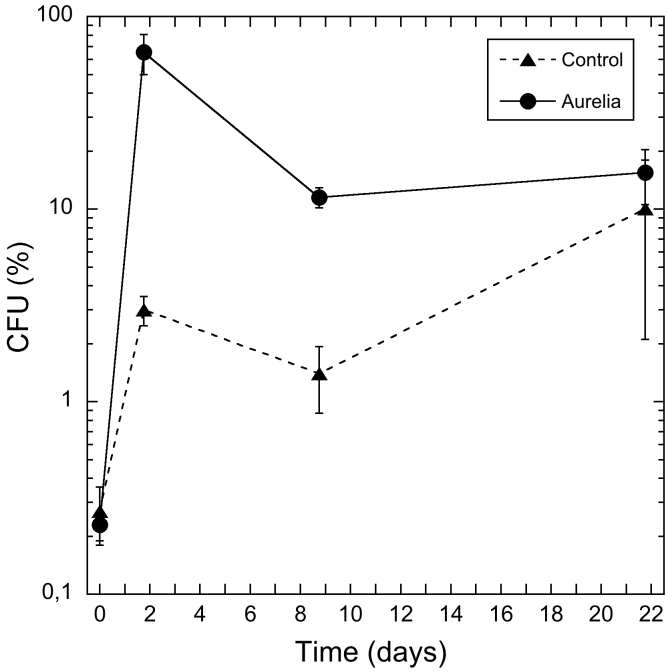
100
10
1
0,1
CFU (%)
0
2
4
6
8
10
12
14
16
18
20
22
Time (days)
Control
Aurelia

Figure 4

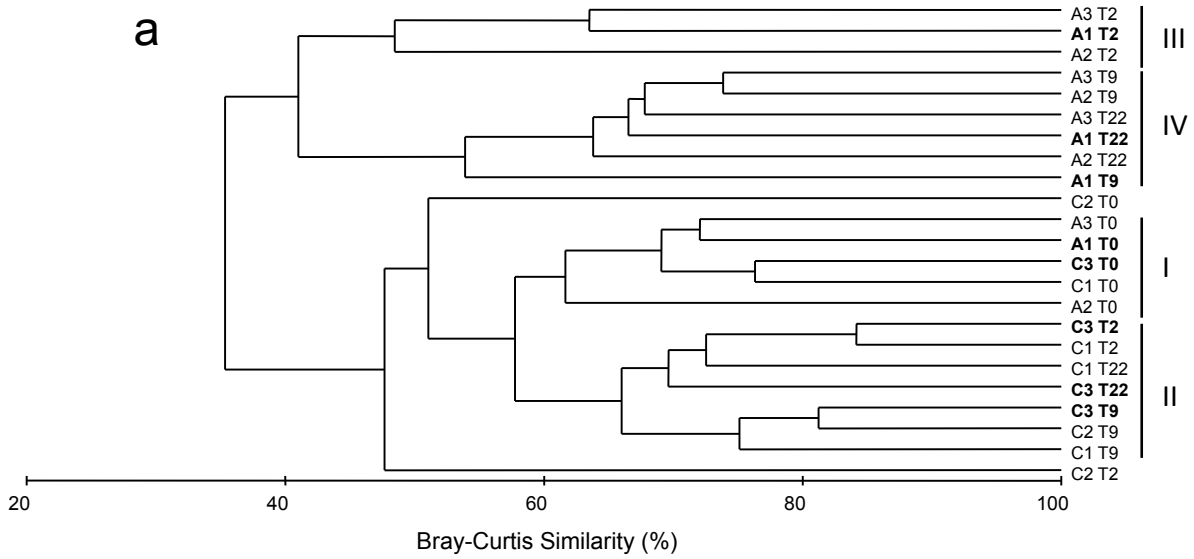
a
A3 T2
A1 T2
A2 T2
A3 T9
A2 T9
A3 T22
A1 T22
A2 T22
A1 T9
C2 T0
A3 T0
A1 T0
C3 T0
C1 T0
A2 T0
C3 T2
C1 T2
C1 T22
C3 T22
C3 T9
C2 T9
C1 T9
C2 T2
III
IV
I
II
20
40
60
80
100
Bray-Curtis Similarity (%)

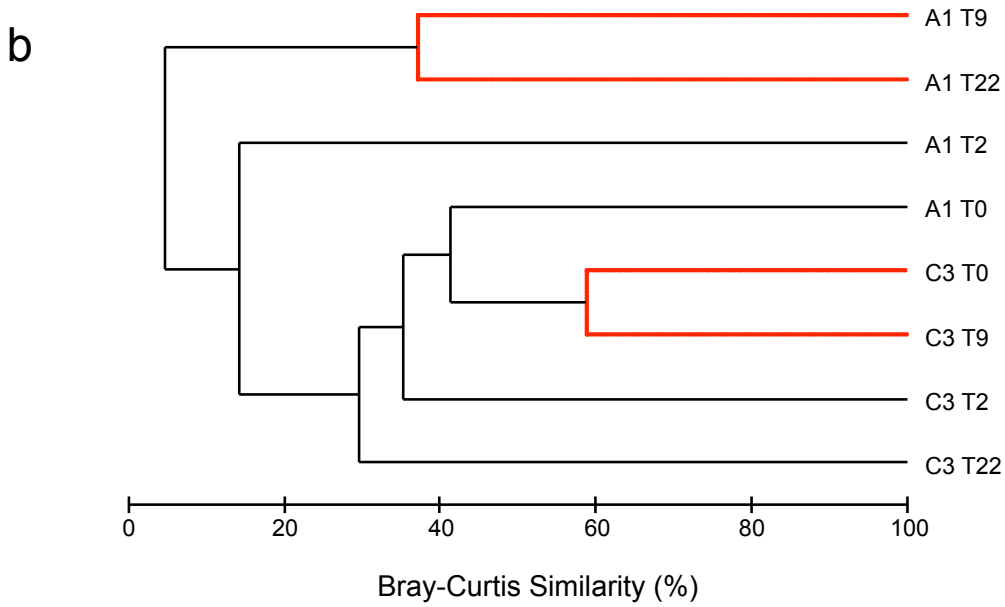
b
A1 T9
A1 T22
A1 T2
A1 T0
C3 T0
C3 T9
C3 T2
C3 T22
0
20
40
60
80
100
Bray-Curtis Similarity (%)

Figure 5

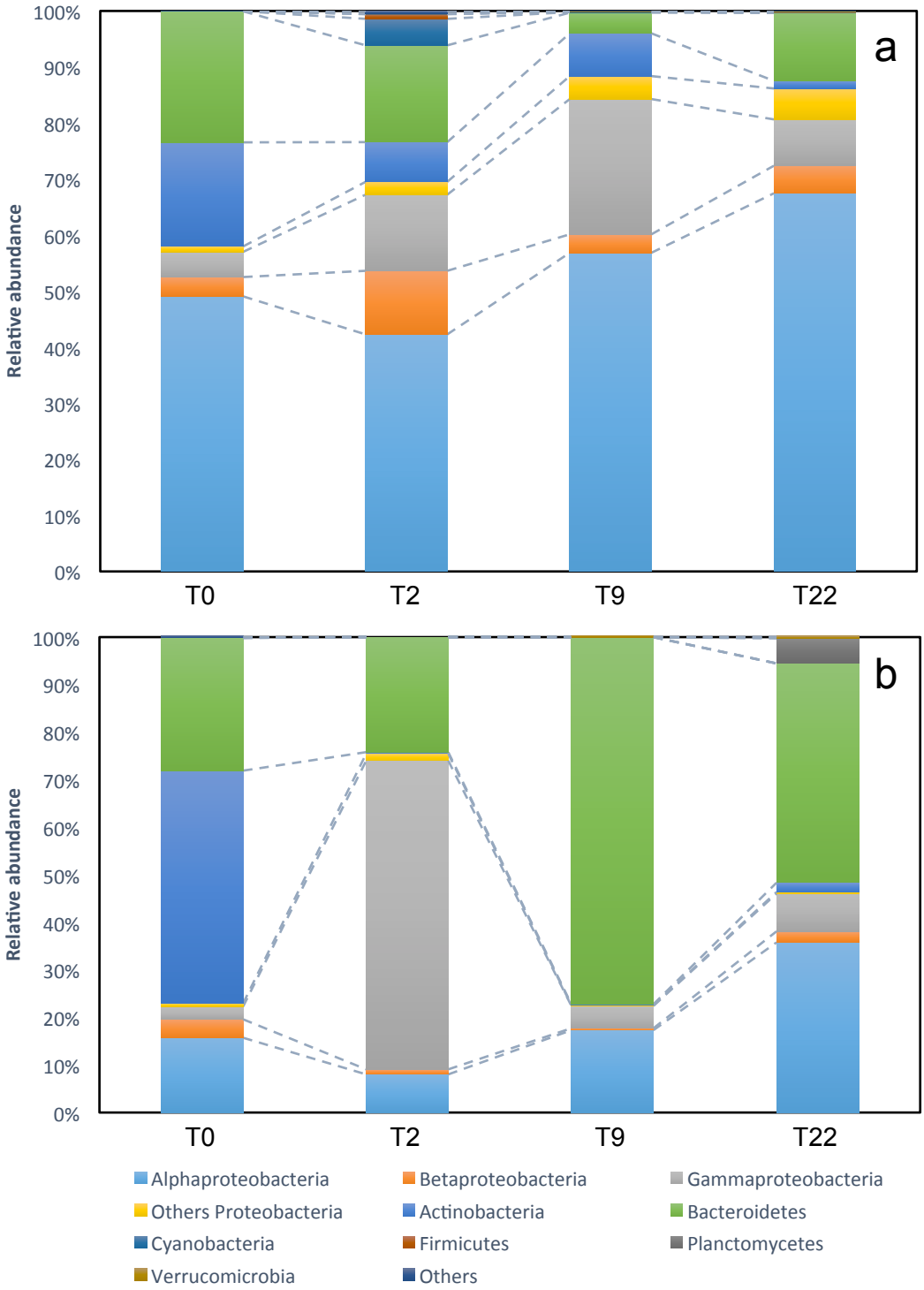
a
b
Relative abundance
100%
90%
80%
70%
60%
50%
40%
30%
20%
10%
0%
T0
T2
T9
T22
Alphaproteobacteria
Betaproteobacteria
Gammaproteobacteria
Others Proteobacteria
Actinobacteria
Bacteroidetes
Cyanobacteria
Firmicutes
Planctomycetes
Verrucomicrobia
Others

Figure 6

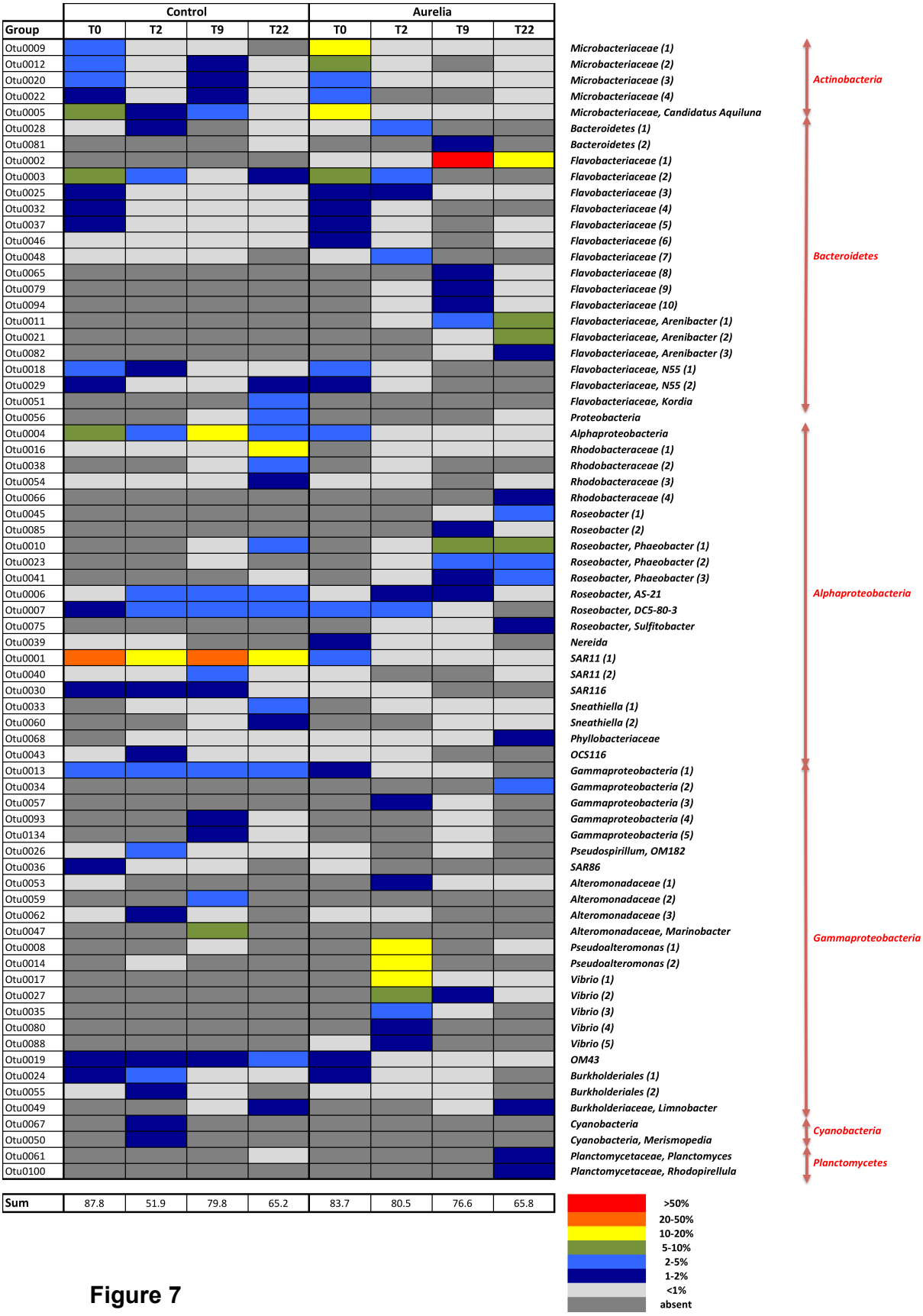
Control
Aurelia
Group
T0
T2
T9
T22
Otu0009
Otu0012
Otu0020
Otu0022
Otu0005
Otu0028
Otu0081
Otu0002
Otu0003
Otu0025
Otu0032
Otu0037
Otu0046
Otu0048
Otu0065
Otu0079
Otu0094
Otu0011
Otu0021
Otu0082
Otu0018
Otu0029
Otu0051
Otu0056
Otu0004
Otu0016
Otu0038
Otu0054
Otu0066
Otu0045
Otu0085
Otu0010
Otu0023
Otu0041
Otu0006
Otu0007
Otu0075
Otu0039
Otu0001
Otu0040
Otu0030
Otu0033
Otu0060
Otu0068
Otu0043
Otu0013
Otu0034
Otu0057
Otu0093
Otu0134
Otu0026
Otu0036
Otu0053
Otu0059
Otu0062
Otu0047
Otu0008
Otu0014
Otu0017
Otu0027
Otu0035
Otu0080
Otu0088
Otu0019
Otu0024
Otu0055
Otu0049
Otu0067
Otu0050
Otu0061
Otu0100
Microbacteriaceae (1)
Microbacteriaceae (2)
Microbacteriaceae (3)
Microbacteriaceae (4)
Microbacteriaceae, Candidatus Aquiluna
Bacteroidetes (1)
Bacteroidetes (2)
Flavobacteriaceae (1)
Flavobacteriaceae (2)
Flavobacteriaceae (3)
Flavobacteriaceae (4)
Flavobacteriaceae (5)
Flavobacteriaceae (6)
Flavobacteriaceae (7)
Flavobacteriaceae (8)
Flavobacteriaceae (9)
Flavobacteriaceae (10)
Flavobacteriaceae, Arenibacter (1)
Flavobacteriaceae, Arenibacter (2)
Flavobacteriaceae, Arenibacter (3)
Flavobacteriaceae, N55 (1)
Flavobacteriaceae, N55 (2)
Flavobacteriaceae, Kordia
Proteobacteria
Alphaproteobacteria
Rhodobacteraceae (1)
Rhodobacteraceae (2)
Rhodobacteraceae (3)
Rhodobacteraceae (4)
Roseobacter (1)
Roseobacter (2)
Roseobacter, Phaeobacter (1)
Roseobacter, Phaeobacter (2)
Roseobacter, Phaeobacter (3)
Roseobacter, AS-21
Roseobacter, DC5-80-3
Roseobacter, Sulfitobacter
Nereida
SAR11 (1)
SAR11 (2)
SAR116
Sneathiella (1)
Sneathiella (2)
Phyllobacteriaceae
OCS116
Gammaproteobacteria (1)
Gammaproteobacteria (2)
Gammaproteobacteria (3)
Gammaproteobacteria (4)
Gammaproteobacteria (5)
Pseudospirillum, OM182
SAR86
Alteromonadaceae (1)
Alteromonadaceae (2)
Alteromonadaceae (3)
Alteromonadaceae, Marinobacter
Pseudoalteromonas (1)
Pseudoalteromonas (2)
Vibrio (1)
Vibrio (2)
Vibrio (3)
Vibrio (4)
Vibrio (5)
OM43
Burkholderiales (1)
Burkholderiales (2)
Burkholderiaceae, Limnobacter
Cyanobacteria
Cyanobacteria, Merismopedia
Planctomycetaceae, Planctomyces
Planctomycetaceae, Rhodopirellula
Actinobacteria
Bacteroidetes
Alphaproteobacteria
Gammaproteobacteria
Cyanobacteria
Planctomycetes
Sum
87.8
51.9
79.8
65.2
83.7
80.5
76.6
65.8
>50%
20-50%
10-20%
5-10%
2-5%
1-2%
<1%
absent

Figure 7

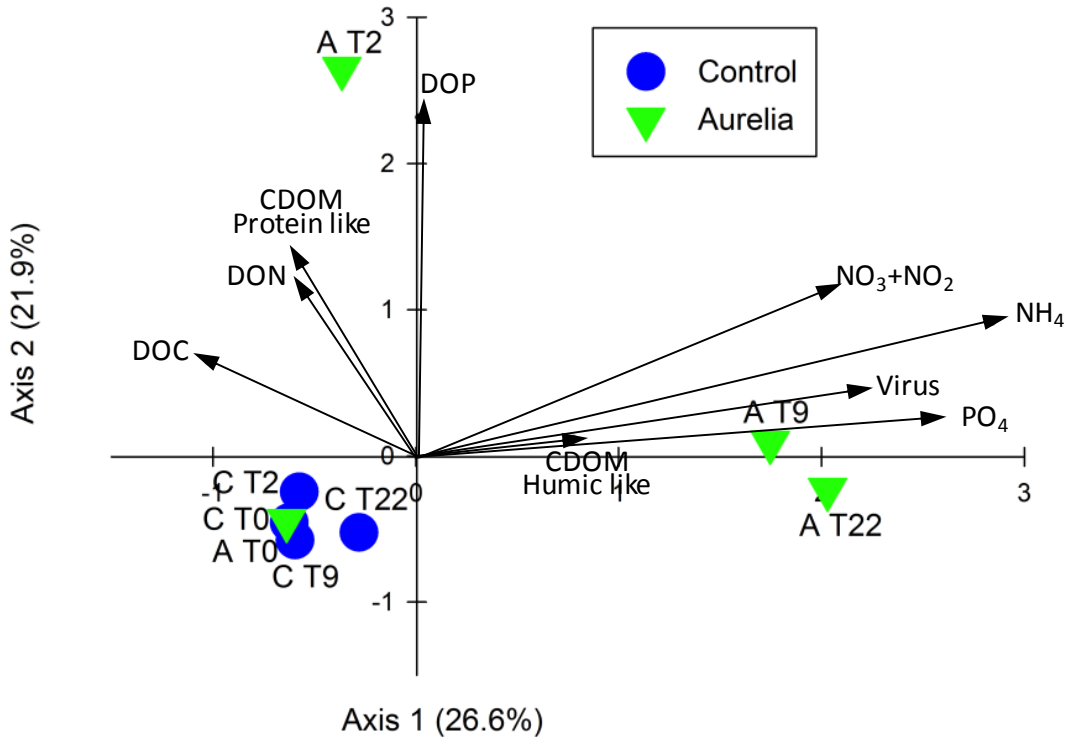
A T2
DOP
Control
Aurelia
CDOM
Protein like
DON
DOC
NO3+NO2
NH4
Virus
A T9
PO4
CDOM
Humic like
C T2
C T22
C T0
A T0
C T9
A T22
Axis 2 (21.9%)
Axis 1 (26.6%)
3
2
1
0
-1
-1
0
3

Figure 8

Supplementary information

Table S1. Inflation factor of CCA analysis. A value close to 1 indicates no redundancy with other variables. mc: multicolinearity between variables.

Variable	Inflation factor
NO3 + NO2	mc
NH4	7.84
PO4	mc
DOC	28.81
DON	85.03
DOP	30.77
CDOM Fluo - Protein like	245.5
CDOM Fluo - Humic like	8.07
Virus	6.89

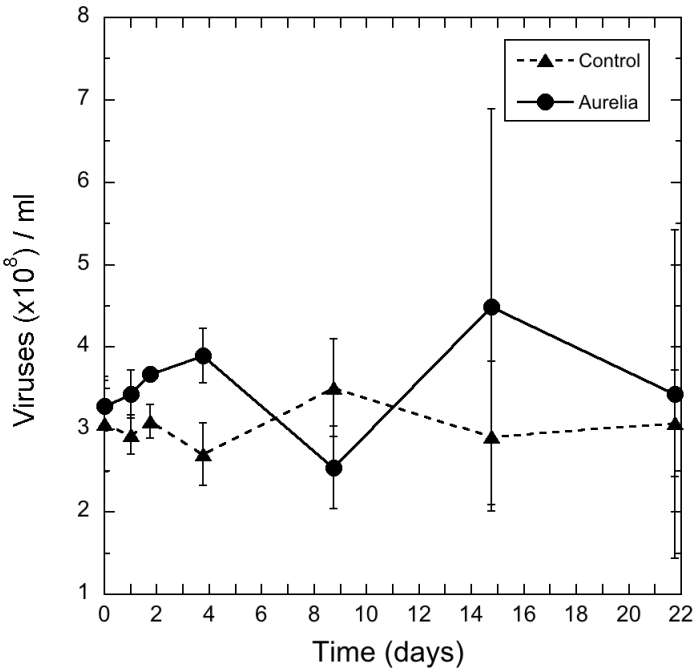

Fig. S1. Virus concentration during the incubations. Each point represents 3 replicates (mean ± standard deviation).

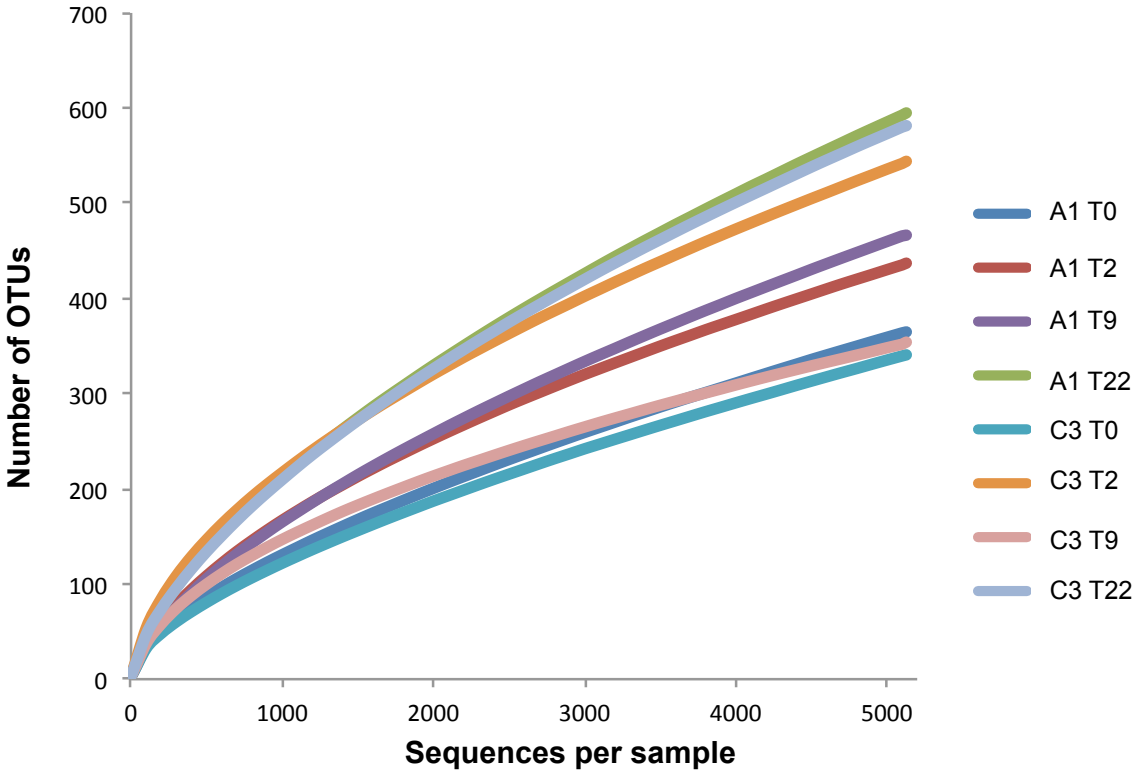

Fig. S2. Rarefaction curves of observed operational taxonomic units (OTU) based on 16S rRNA sequences retrieved from the different samples.